# Properties of UNS S32760 Duplex Stainless Steels Powders and L-PBF Components as Function of Different Processing Gases

J. Jpn. Soc. Powder Powder Metallurgy, **72** (2025) S587-S591
https://doi.org/10.2497/jjspm.15C-T1-27



# Properties of UNS S32760 Duplex Stainless Steels powders and L-PBF components as function of different processing gases

Federico Simone Gobber[1]*, Antonio Pennacchio[1] and Marco Actis Grande[1]

[1]Politecnico di Torino – DISAT, Viale T. Michel 5, Alessandria, 15121, Italy.

**Abstract**
Super duplex stainless steels (SDSS) combine the advantages of ferritic and austenitic steels and reach an excellent combination of mechanical and corrosion properties. The paper focuses on the production of UNS S32760 (X2CrNiMoCuWN25-7-4, AISI F55, 1.4501) SDSS powders through Vacuum induction melting Inert Gas Atomization (VIGA) with different gas atmospheres, Argon or Nitrogen. The effect of the different gases used during the melting and the atomizing on the characteristics of the final powder was investigated, in terms of granulometry, morphology, microstructure, chemical composition (also taking into account light elements such as N, O, H, C, and S). Powders were then processed by means of Laser Powder Bed Fusion (L-PBF) and microstructural features and mechanical properties of produced components were analyzed in the as processed state and after thermal treatments, properly optimized to obtain a good balancing between the α ferrite/austenite phases.

**Keywords:** gas atomization, super duplex steels, L-PBF

## Introduction

Modern duplex stainless steels (DSS) and super duplex stainless steel (SDSS) consist of a microstructure containing approximately equal proportions of austenite and ferrite, providing a combination of high strength from the ferrite phase with the ductility and toughness of the austenite phase. The addition of nitrogen improves the distribution of elements between the two phases, enhances the strength of austenite, improves corrosion resistance, and enhances weldability, among other benefits [1, 2]. This unique microstructure imparts superior corrosion resistance, especially in chloride stress corrosion and chloride pitting corrosion, and enhances strength compared to the most commonly used austenitic stainless steels like AISI 304 or AISI 316.
Duplex stainless steels are commonly used due to their excellent resistance to stress corrosion cracking (SCC) [3, 4], as well as good corrosion resistance in various environments. Their high strength and hardness also provide resistance to erosion-corrosion [5], cavitation [6], and corrosion fatigue [7, 8].

The main objective of this research is to investigate the effect of two different melt chamber gas atmospheres, Ar or N2, on the nitrogen content of the SDSS UNS S32760 powders produced by Vacuum Induction Melting Inert Gas Atomization (VIGA) using metal scraps. Additionally, the study aims to evaluate the impact of different atomisation gases, Ar or N2, on the properties of the powders, including granulometry, morphology, microstructure, chemical composition (including light elements such as O, N, H, C, and S). The identification of optimal gas process parameters for producing UNS S32760 powders with the correct composition, particularly in terms of nitrogen content, is critical for subsequent processing techniques such as Laser Powder Bed Fusion (L-PBF), and Metal Injection Molding (MIM), as it significantly impacts the pitting resistance and the balance of the α ferrite/austenite phase, which is crucial for the mechanical properties of the final product.

## Materials and methods

In the current investigation, four batches of forging raw material scraps of UNS S32760 super duplex stainless steel (SDSS) with an approximate weight of 6.5 ± 0.1 kg were prepared for gas atomisation using a Vacuum Induction Gas Atomization (VIGA) atomiser.

The chemical composition of the starting material was determined by optical emission spectroscopy (OES) before loading the SDSS into the crucible (Tab. 1). Not reported in the tab., Phosphorus was measured below 0.02 %wt and sulphur at 0.004 %wt (in the standard BS EN 10088-2-2014 are 0.035 wt% for P and 0.015 wt% for S as maximum allowed values).
After evacuating the atomiser to a pressure of 6*10-3 mbar, the material was gradually heated using an induction heater at a rate of 18 ± 4°C/min to avoid thermal shocks to the alumina crucible. The induction process was carried out under the following parameters: power ranging from 3 to 12 kW, frequency ranging from 6 to 7 kHz, and voltage ranging from 110 to 200 V.

When reaching a temperature of approximately 1000°C, the two chambers were filled (to prevent the loss of volatile elements from the molten pool) with the process gases selected according to the experimental test combination in progress, which involved the use of either argon or nitrogen gas in both the melting and atomising chambers, or the use of argon gas in the atomising chamber and nitrogen as the atomisation gas, and vice versa; for a total of four different process modes.

*corresponding author, E-mail: federico.gobber@polito.it

Tab. 1: Wrought material composition as measured by OES, in comparison to the chemical composition of UNS S32760 in accordance with the standard BS EN 10088-2-2014

| AISI F55 | C | Si | Mn | Cr | Mo | Ni | Cu | Co | Nb | Ti | V | W | N | Fe |
|---|---|---|---|---|---|---|---|---|---|---|---|---|---|---|
| BS EN 10088-2-2014 | ≤ 0.030 | ≤ 1 | ≤ 1 | 24.0 to 26.0 | 3.0 to 4.0 | 6.0 to 8.0 | 0.50 to 1.0 | - | - | - | - | 0.50 to 1.0 | 0.20 to 0.30 | bal |
| Wrought material | 0.015 ± 0.001 | 0.406 ± 0.001 | 0.628 ± 0.003 | 25.8 ± 0.03 | 3.6 ± 0.01 | 7.15 ± 0.03 | 0.65 ± 0.01 | 0.065 ± 0.001 | 0.02 | < 0.001 | 0.06 ± 0.008 | 0.65 ± 0.025 | 0.20 ± 0.007 | bal |

Subsequently, the atomisation chamber was set to atmospheric pressure while a slightly higher pressure of 0.05 barg with a fluxing atmosphere was maintained in the melt chamber. Before starting the atomisation process, the pressure in the melt chamber was increased to 0.25 barg to facilitate the flow of molten metal into the atomisation chamber. During atomisation, the oxygen level in the atomisation chamber was measured and found to be below 5 ppm (using a Cambridge Sensotec - Rapidox 1100 Zr). Independently from the atomisation gas used, Ar or N2, the atomisation pressure was set to 40 bar. Most of the atomised powders were accumulated in the primary hopper, ranging from 6.1 to 6.4 kg. A minor portion of the powders was separated from the exhaust gas (Ar or N2) through a cyclone and then collected in a secondary hopper with a weight range of 0.15 to 0.3 kg. The atomisation efficiency was assessed by dividing the total mass of powders collected from both primary and secondary hoppers by the initial mass of the material loaded into the alumina crucible.

The powders obtained from each atomisation were thoroughly mixed to ensure uniform distribution and prevent any potential segregation effects. Subsequently, the powders were sieved with a 250 µm mesh size to eliminate any debris generated during atomisation.

Following atomisation, three sets of samples were obtained from each of the four different gas process combinations (Ar or N2) for analysis using Leco CS 744 and Leco ONH 836 techniques to quantify the content of interstitials and light elements (O, N, H, C, and S). Powder size distribution (PSD) was determined by measuring the dry samples using laser-granulometry (Mastersizer 3000) with 15% feed and 3.0 bar carrier gas, while assuming spherical powders and utilising the coefficient of reflectivity appropriate for stainless steel from the Malvern datab.ase. Qualitative characterisation of the powder morphology was carried out on powders with a size below 150 µm using scanning electron microscopy (SEM – Zeiss EVO 15). The amounts of austenite/ferrite in the powders and wrought material were determined by XRD. A PULSTEC µ-X360s diffractometer devoted to measuring residual stresses and retained austenite was employed; the instrument has a Cr anode working at 30 kV - 1.5 mA and is equipped with a 2D detector. The analysis was reduced to the 120 – 175° 2θ interval.

**Results and discussion**

A gross process yield of 97.4% was achieved in all operational cases. In addition, the yield within the particle size range of 20-63 µm was between 35-40% for all combinations of process gases employed. In the Tab. 2 are presented the percentage of O, N, and H detected in the powders using different combinations of process gases for each relevant particle size range. In all experimental tests, the carbon content in the powders (not reported in Tab. 2) exhibits a slight increase compared to the wrought material, yet it remains well within the compositional range (0.02 - 0.03 wt%); while the sulfur content has been observed to be below 10 ppm.

Tab. 2. Light elements concentrations in UNS S32760 powders atomised using different combinations of process gases.

| **Melting chamber atmosphere** | **Atomizing gas** | **Powder size** | **O [%wt]** | **N [%wt]** | **H [ppm]** |
|---|---|---|---|---|---|
| Ar | Ar | <20 µm | 0.0538 ± 0.0058 | 0.214 ± 0.001 | 12.2 ± 3.00 |
| | | 53 – 63 µm | 0.0193 ± 0.0004 | 0.159 ± 0.001 | 3.62 ± 1.44 |
| | | 106 – 125 µm | 0.0163 ± 0.0002 | 0.153 ± 0.002 | 1.33 ± 2.17 |
| $N_2$ | $N_2$ | <20 µm | 0.0340 ± 0.0007 | 0.473 ± 0.004 | 6.80 ± 1.85 |
| | | 53 – 63 µm | 0.0215 ± 0.0001 | 0.479 ± 0.002 | 1.88 ± 3.06 |
| | | 106 – 125 µm | 0.0210 ± 0.0002 | 0.479 ± 0.005 | 2.00 ± 1.21 |

The data presented in Tab. 2 show how the nitrogen content varies depending on the combinations of argon or nitrogen as process gas:

- Using argon in the melt chamber and as atomising gas decreased the nitrogen content in the atomised powders compared to the feedstock material (Tab. 2) while using nitrogen in atomisation is sufficient to hinder such decrease.
- The application of nitrogen as both the cover gas in the atomisation chamber and the atomising gas led to an increase in the nitrogen content of 0,260 wt% compared to the feedstock material. A slightly lower increment was observed when nitrogen was used as the cover gas and argon was employed as the atomising gas.
- No significant differences in nitrogen content were found in relation to the three different particle size ranges examined for each combination of process gases used.

The oxygen contents, as expected, showed no changes based on the different combinations of process gases employed; their variation is mainly determined by the powder size, with a higher oxygen content observed for small powders.
In some cases, the average hydrogen content was below the instrument's detection limits, based on its calibration parameters at the time of analysis, n.a values reported in Tab. 2.

The SEM images presented in Fig. 1 show the morphology of powders obtained combining the process gases. For each case, both low and high magnification images are provided. The powders subjected to electron microscopy examination were sieved with a 250 µm mesh.
No significant morphological differences are evident as a consequence of using argon or nitrogen as atomisation gas. In both cases, powders with high sphericity and low satellite presence were obtained.

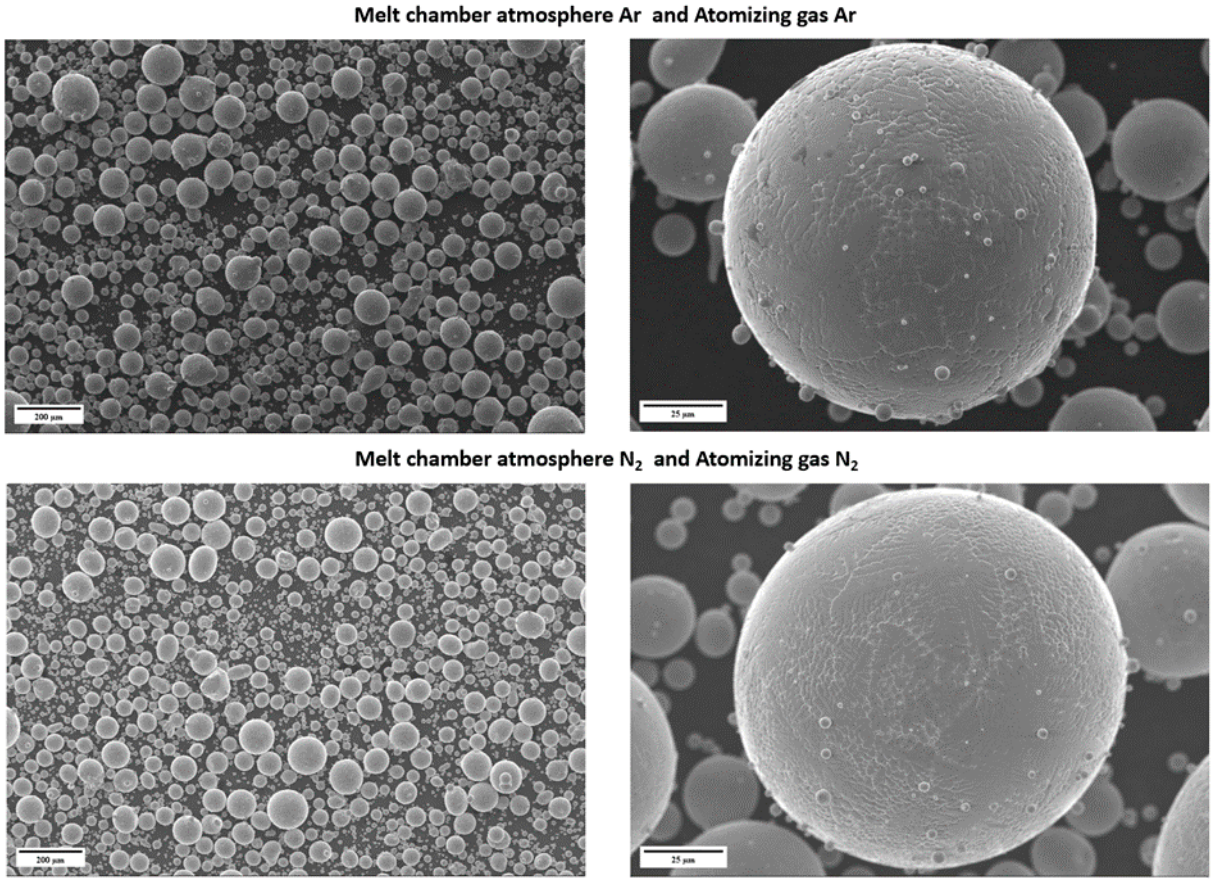


Fig. 1. Secondary electron SEM images of the gas-atomised powders (sieved with a 250 µm mesh) atomised using different process gas combinations in the melting chamber and as the atomisation gas, respectively from top to bottom: Ar/Ar and N2/N2 were employed as process gas combinations in the melting chamber and as atomisation gases.

The microstructures of samples manufactured through L-PBF and heat treated to 1080°C are presented in Fig. 2. As expected, an higher amount of argon leads to an increase in the ferrite fraction, that after heat treatment is around 58% (Fig. 2a). Conversely the material manufactured from nitrogen atomized powders is richer in austenite after heat treating at 1080°C, more precisely around 59% austenite (Fig. 2b). The microstructures of the two alloys are different even comparing the size of the austenitic and ferritic domains at the same magnification. A coarser microstructure is characteristic for the low nitrogen material (argon atomized powders) with austenite having both lamellar and globular morphology based on the nucleation site (either border of the melt pool or inside the melt pool). A finer microstructure is characteristic for high nitrogen alloy (nitrogen atomized powders) with austenitic and ferritic

domains more similar in size. The austenite/ferrite ratio falls within the acceptance interval only for the alloys nitrogen atomized powders with a final amount of 58% as measured by XRD analysis.

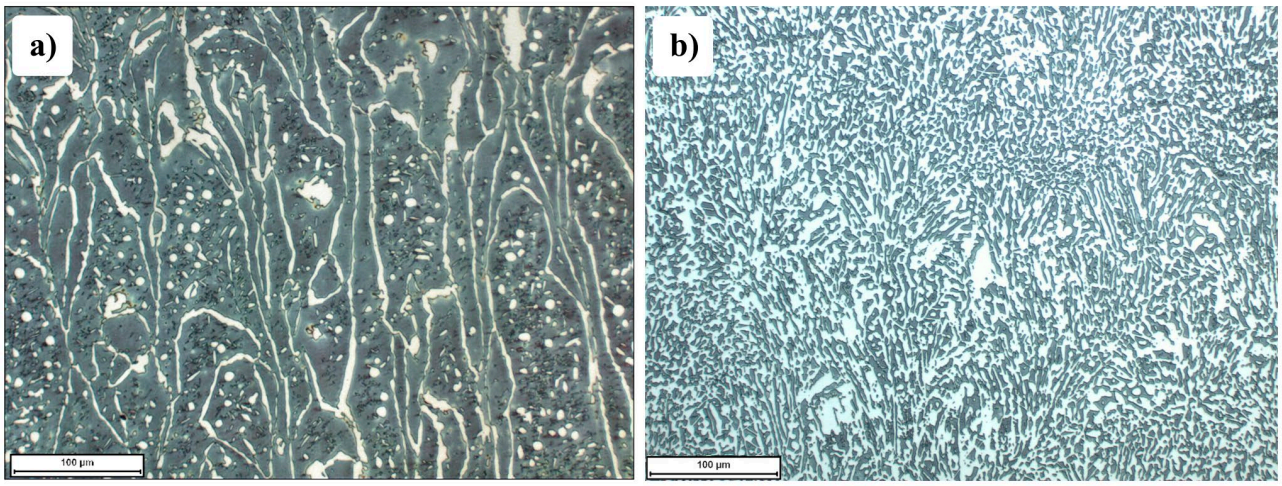


Fig. 2. Light optical micrograph of samples manufactured by L-PBF and heat treated to 1080°C. a) sample from Ar melt/atomized powders, sample from $N_2$ melt/atomized powders.

**Conclusion**

This study presents the production of super duplex UNS S32760 steel powders through close-coupled vacuum inert gas atomisation, with a focus on analysing the effect of different process gas on the final nitrogen content of powders and the final austenite/ferrite ratio for samples produced by laser powder bed fusion.

Using argon for both melting and atomisation leads to a reduction in nitrogen content of 0,05%wt compared to the starting feedstock material. The use of nitrogen as both the cover gas in the melting chamber and as the atomising gas resulted in an increase in nitrogen content equivalent to 0,260 %wt if compared to the wrought material.

The use of argon in the melt chamber resulted in fully ferritic powders with cellular/dendritic solidification morphologies, depending on the size of the analysed powders. Replacing argon with nitrogen in the melting chamber results in the production of powders with an austenite content in the range of approximately 25% wt; nevertheless the use of nitrogen as the atomisation gas does not significantly affect the austenite content in the powders.

A heat treatment is necessary after L-PBF to reach an acceptable partitioning between austenite and ferrite. A final amount of 41% austenite was obtained for argon atomized powders while 58% austenite was achieved starting from nitrogen atomized powders.

**References**

1) Lizlovs, E.A. Corrosion Resistance of Some Commercial Duplex Stainless Steels; Climax Molybdenum Report RP-33-80-08; Climax Molybdenum: Fort Madison, IA, USA, 1981.
2) Foct, J.; Magnin, T.; Perrot, P.; Vogt, J.-B. Nitrogen Alloying of Duplex Stainless Steels. In Duplex Stainless Steels '91; Les Editions de Physique: Les Ulis, France, 1991.
3) Tsai, W.T.; Chen, M.S. Stress corrosion cracking behavior of 2205 duplex stainless steel in concentrated NaCl solution. Corros. Sci. 2000, 42, 545–559, doi:10.1016/S0010-938X(99)00105-5.
4) Liou, H.Y.; Hsieh, R.I.; Tsai, W.T. Microstructure and stress corrosion cracking in simulated heat- affected zones of duplex stainless steels. Corros. Sci. 2002, 44, 2841–2856, doi:10.1016/S0010- 938X(02)00068-9.
5) Neville, A.; Hodgkiess, T.; Dallas, J.T. A study of the erosion-corrosion behaviour of engineering steels for marine pumping applications. Wear 1995, 186–187, 497–507, doi:10.1016/0043- 1648(95)07145-8.
6) Hänninen, H.; Romu, J.; Ilola, R.; Tervo, J.; Laitinen, A. Effects of processing and manufacturing of high nitrogen-containing stainless steels on their mechanical, corrosion and wear properties. J. Mater. Process. Technol. 2001, 117, 424–430, doi:10.1016/S0924-0136(01)00804-4.
7) Tseng, C.M.; Liou, H.Y.; Tsai, W.T. The influence of nitrogen content on corrosion fatigue crack growth behavior of duplex stainless steel. Mater. Sci. Eng. A 2003, 344, 190–200, doi: 10.1016/S0921-5093(02)00404-5.
8) Khoshnaw, F., Marinescu, C., Sofronia, A., Munteanu, C., Marcu, M., Barbulescu, L. E., ... & Paraschiv, A. (2021). Microstructural and thermoanalytical characterisation of super duplex stainless steel-UNS S32760-F55. Materials Today Communications, 28, 102644.
9) Trydell, K., Persson, KA., Fuertes, N. et al. Ferrite fraction in duplex stainless steel welded with a novel plasma arc torch. Weld

World 67, 805–817 (2023).
10) Migiakis, K., Papadimitriou, G.D. Effect of nitrogen and nickel on the microstructure and mechanical properties of plasma welded UNS S32760 super-duplex stainless steels. J Mater Sci 44, 6372–6383 (2009).

Received July 1, 2024; Revised July 1, 2024; Accepted August 20, 2024